



Study of the inhibition effects on glutathione peroxidase immobilized on MNPs using a stopped-flow microfluidic system

Vanesa Román-Pizarro¹ · Alba María Carrión-Escudero¹ · Ángela Écija-Arenas¹ · Juan Manuel Fernández-Romero¹

Received: 31 October 2022 / Revised: 30 November 2022 / Accepted: 4 January 2023 / Published online: 18 January 2023
© The Author(s) 2023, corrected publication 2023

Abstract

A stopped-flow microfluidic system to monitor glutathione peroxidase (GPx) activity and evaluate potential inhibitors of the enzyme has been developed based on the integration of the microfluidic chip in the reaction/detection zone. This integration supposes the physical alignment at the optimal location of the microfluidic channel, both the magnetically retained enzyme microreactor (MRE μ R) and the remote luminescence detection using a focused bifurcated fiber optic bundle (BFOB) connected to a conventional spectrofluorometer detector. The method is based on the coupling of two competitive oxidative chemical reactions, in which glutathione (GSH) and homovanillic acid (HVA) competed for their interaction with hydrogen peroxide in the presence of the magnetically retained GPx-MNPs. The biocatalytic reaction was followed by monitoring the fluorescence of the biphenyl-HVA dimer formed. The dynamic range of the calibration graph was 0.45–10 $\mu\text{mol L}^{-1}$, expressed as GSH concentration with a detection limit of 0.1 $\mu\text{mol L}^{-1}$ ($r^2=0.9954$, $n=10$, $r=3$). The precision expressed as the relative standard deviation (RSD%) was between 0.5 and 3.9%. The stopped-flow microfluidic system showed a sampling frequency of 25 h^{-1} . The method was applied to the study of GPx inhibition provided by three inhibitory compounds, two metallic ions Hg(II) and Cu(II) and t-butyl hydroperoxide, and their presence in liquid samples, as water, milk, and edible oil. Recovery values between 88.7 and 99.4% were achieved in all instances.

Keywords Glutathione peroxidase · Stopped-flow microfluidic · Enzyme-magnetic nanoparticles · Bifurcated fiber optic fluorimetry · Competitive redox reaction · Metallic ions and hydroperoxide as inhibitors

Introduction

Several analytical methods have been based on kinetic systems applying enzymes in solution and immobilized in areas such as clinical biochemistry [1–5]. Some of the characteristics inherent to developing analytical determinations based on the use of enzymes are sensitivity and selectivity. However, one of the most significant limitations is the cost of its use in the solution. Therefore, enzyme immobilization is supposed some advantages, such as reusability, resistance to moderate changes in pH, temperature, or ionic strength of the medium, and the ability to maintain the enzymatic activity stable over time [6–8]. The immobilization of enzymes on inert supports and their localization in small reactors in the reaction/detection zone is the most common way to incorporate enzymatic biocatalysts in continuous automatic analysis systems. These have been arranged in the form of reactors with immobilized enzymes using controlled pore glass (IMER) or, more recently, by magnetic

Published in the topical collection *Analytical Nanoscience and Nanotechnology* with guest editors Ángel Ríos and Wolfgang J. Parak.

In honor of Prof. Miguel Valcárcel.

✉ Juan Manuel Fernández-Romero
qa1feroj@uco.es

Vanesa Román-Pizarro
q52ropiv@uco.es

Alba María Carrión-Escudero
b42caesa@uco.es

Ángela Écija-Arenas
q92ecara@uco.es

¹ Departamento de Química Analítica, Instituto Universitario de Investigación en Química Fina Y Nanoquímica (IUNAN), Universidad de Córdoba, Edificio Anexo “Marie Curie”, Campus de Rabanales, 14071 Córdoba, Spain

retention technology in the form of a magnetically retained enzyme reactor (MRE_R). In case the flow systems consisted of microfluidic, the dimensions of the reactor decrease, considering the magnetically retained enzyme microreactor (MRE_μR). To obtain this type, enzymes were immobilized on magnetic nanoparticles (MNPs) [9, 10].

The use of enzymes with peroxidase activity has been widely used in the field of analytical chemistry when they are incorporated as immobilized biocatalysts [11]. Usually, these enzymes with peroxidase activity catalyze the oxidation of organic and inorganic compounds in the presence of hydrogen peroxide (H₂O₂), which acts as an oxidant. The enzyme glutathione peroxidase (glutathione:hydrogen-peroxide oxidoreductase; EC1.11.1.9, GPx) is an enzyme belonging to the family of seleno-proteins that catalyzes the reduction of peroxides using glutathione (GSH) as a reductor [12]. The GPx enzyme is one of the most important within this group of enzymes due to its role as an antioxidant in defense as a protector against reactive oxygen species (ROS) [13, 14].

For the determination of glutathione in biological fluids, different photometric-enzymatic methods have been proposed using the immobilized GPx enzyme [15]. On the other hand, several methods have been developed that involve the characterization of activators and inhibitors of the GPx enzyme, and these methods can be enzymatic with fluorometric detection or photometric [16–19]. Many of them involve the determination of GPx inhibitors by vitamins, metals, cysteine, selenite, and hydroperoxides [20–26]. The most used method for determining inhibitors of the GPx enzyme is based on the photometric monitoring of the oxidation of GSH to GSSG [22].

In this work, an auxiliary reaction was used to carry out the fluorimetric monitoring of the enzymatic reaction. The signal obtained with this reaction indicates the competitive reaction with the analytical reaction catalyzed by the enzyme glutathione peroxidase. The oxidation of homovanillic acid (HVA) with H₂O₂ has been used as a secondary reaction [27, 28].

Finally, the development of this enzymatic method at microfluidic size has been performed by using an on-flow integrated stopped-flow mode, given its usefulness in the development of kinetic-enzymatic methodologies in clinical biochemistry, especially those in which biocatalysts have been immobilized. Microfluidic devices are supposed an alternative to reduce enzyme consumption and ease immobilization [29]. The integrated microfluidic system is based on the on-flow stopped-flow kinetic model, in which the GPx-MNPs complex has been magnetically retained in the reaction/detection zone, where the biocatalytic reaction that competes with the oxidation reaction of HVA took place.

This work demonstrates a method based on a stopped-flow microfluidic system using GPx immobilized in the

reaction/detection zone. The developed microfluidic system has been applied to the determination of glutathione as a substrate for the enzyme glutathione peroxidase and the study of potential glutathione reductase inhibitors in the environment and food samples. In this double system of redox reactions, the substrates of both GSH and HVA reactions compete for their interaction with H₂O₂, and the luminescent signal could be related to the presence of potential inhibitor compounds, such as metals Hg(II) and Cu(II) and the t-butyl hydroperoxide. In the case of the inhibition due to the presence of the metals Cu(II) and Hg(II), the development of the biocatalytic reaction at basic pH conditions induced the formation of metal-enzyme complexes preventing the formation of the enzyme-substrate complex, promoting a competitive inhibition [24, 30]. For t-butyl hydroperoxide, it could be a non-competitive inhibitor since it prevented the GSH oxidation by H₂O₂ at the studied concentration levels, even if it is a substrate of the enzymatic reaction [30, 31].

Materials and methods

Materials

All chemicals used were of analytical grade. Hydrogen peroxide at 30% w/v (H₂O₂), and iron(III) chloride (FeCl₃) were supplied by Panreac (PANREAC Química S.L.U., Barcelona, Spain, <https://www.itwreagents.com/iberia/es/home>). Homovanillic acid (HVA), iron(II) chloride (FeCl₂), N-(3-dimethyl aminopropyl)-N'-ethyl carbodiimide (EDC), glutathione (GSH), tert-butyl hydroperoxide, mercury(II) chloride (HgCl₂), and copper(II) sulfate (CuSO₄) were supplied by Sigma-Aldrich (Merck Life Science S.L.U., Madrid, Spain, <http://www.sigmaaldrich.com/ES/es>). Sodium hydroxide (NaOH), hydrochloric acid (HCl), disodium phosphate, and Tris-HCl were provided by Merck (Merck Life Science S.L.U., Madrid, Spain, <http://www.sigmaaldrich.com/ES/es>). The enzyme glutathione peroxidase (GPx) (EC.1.11.1.9) (glutathione peroxidase from bovine blood erythrocyte samples), with an activity of approximately 300 U mg⁻¹ protein (expressed in DEA units), was also supplied by Sigma-Aldrich.

Apparatus and instruments

All fluorescence signals were acquired using an FL-3000/FM4-3000 bifurcated fiber optic bundle (BFOB) assembled to a Horiba Scientific Fluoromax-4P spectrofluorometer (Horiba Scientific, France, www.horiba.com/scientific/). The information provided by the instrument was processed by FluorEssence Software (HoribaScientific) and OriginPro 2018 64-bit Software (OriginLab Co. 2018, Northampton,

MA). The microfluidic system was adapted to the spectrofluorimeter and aligned to the fiber optic focal point using an x–y–z displacement device (Oriol Instruments, USA, www.newport.com/oriel/). The flow was driven using a Gilson Minipuls-2 peristaltic pump (Gilson Inc., Middleton, UK, www.gilson.com) and a KDS220 syringe pump (KD Scientific Inc., MA, USA, www.kdscientific.com).

As the microfluidic device, a borofloat glass microreactor (H300.015.2) with 15 × 45 mm dimensions and a 2.75 μL internal volume was inserted into a chip holder (FC-PRO. CH4515) (Micronit, Netherlands, www.micronit.com). A lab-built electromagnet facilitated the magnetic retention on the focal point. A Raspberry Pi 3 Model B (Raspberry Pi Foundation, United Kingdom, www.desingspark.com/raspberrypi) as an embedded system has been used to control the electromagnet device using Phyton 3 commands. Two Cheminert VA-CN2 injection valves (Valco, Teknokroma, Barcelona, Spain, www.teknokroma.es) were used to inject both the GPx-MNPs complex and the other reactant solutions. Different polytetrafluoroethylene (PTFE) connections and tubes of 1/16" outer diameter, 250 μm inner diameter, perfluoro-elastomer splints (FFKM), and adequate PEEK connectors have been used.

A conventional oven, an ultrasound bath, and an MPW-350R centrifuge (MPW Med. Instrument, Warsaw, Poland, www.mpw.pl) with a cooling chamber rotating and an angle rotor HSL-11199 (45°, 12 × 12 × 1.5 mL, max. speed = 18,000 rpm, 24,088 × g RCF and $r_{\min}/r_{\max} = 3.5/6.25$) were used for the GPx-MNPs synthesis.

Selection of the enzymatic system

The chemical reaction selected for this study involved the reduction of H₂O₂ to water using the GSH as a reducing compound, which, in turn, competes with the HVA. The analytical reaction studied in this method was the GSH oxidation, but for that, an indicator reaction in which the dimerization of HVA occurred was needed. HVA reaction was used to monitor the reaction by fluorimetry, as shown in Fig. 1. HVA reacted with H₂O₂, giving rise to a fluorescent dimer, with excitation and emission wavelengths of 315 and 425 nm, respectively, at a pH higher than 8 [28]. The decrease in the fluorescence signal can be related to the concentration of peroxide compounds present in the sample.

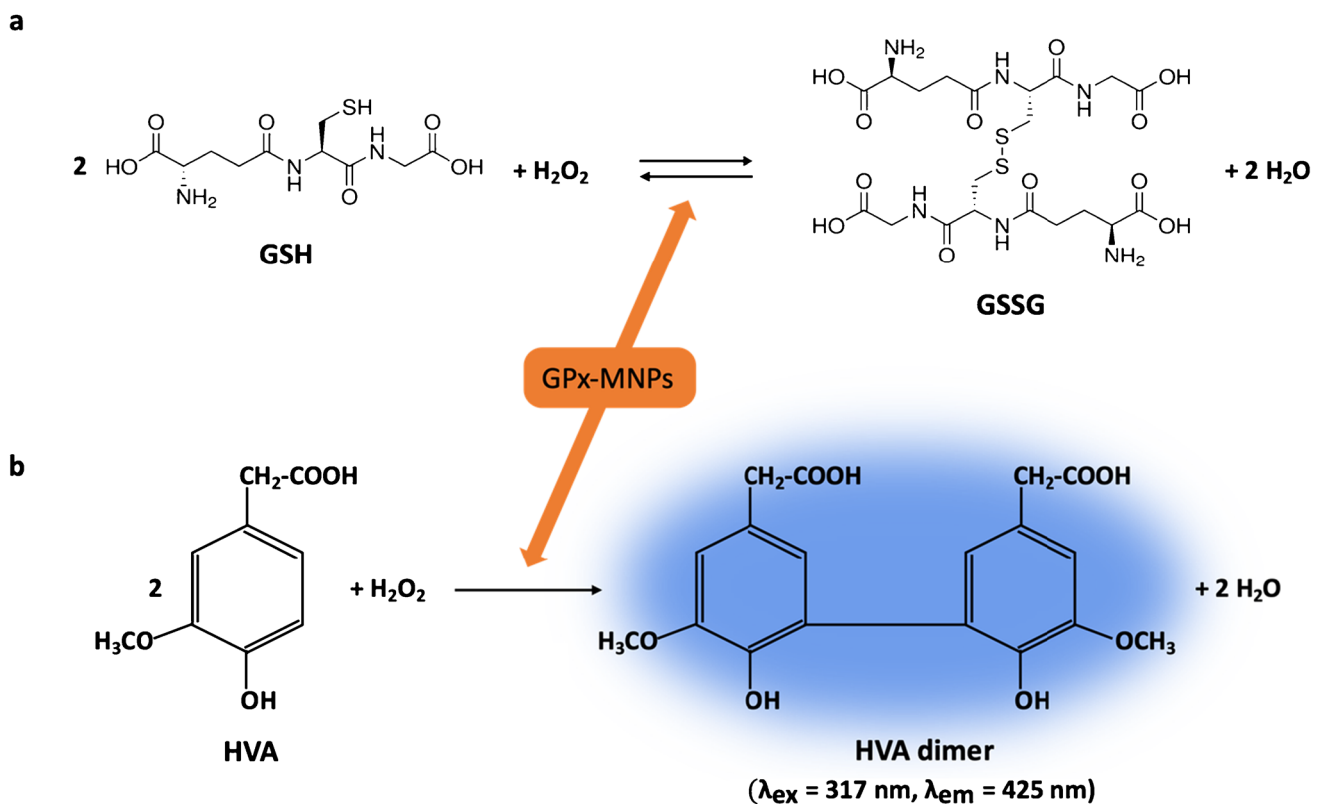


Fig. 1 Reactions involved in the proposed method. **a** Analytical reaction in which glutathione (GSH) oxidation was catalyzed by the glutathione peroxidase (GPx) enzyme to form GSH disulfide (GSSG). **b**

Indicator reaction in which homovanillic acid (HVA) dimer formation occurred for the luminescent monitoring of the enzymatic reaction

Synthesis of GPx-MNPs complex

To perform the synthesis of the GPx-MNPs complex, a previous step for the MNPs synthesis was needed. This synthesis was carried out using the previously described co-precipitation method [32]. Before their use for enzyme immobilization, the solvent was evaporated until completely dried in an oven at 90 °C until the weight remained constant in five successive weightings. The immobilization of the GPx enzyme was carried out by a covalent binding using the cross-linking carbodiimide reaction, which modified the immobilization of other enzymes [8, 33, 34]. Initially, 0.0498 g of dried MNPs were added to 1 mL of phosphate buffer (50 mmol L⁻¹, pH 7.4), and the solution was sonicated for 15 min after adding 0.5 mL of a 0.02 g mL⁻¹ EDC solution dissolved in the phosphate buffer mentioned. After this, 2 mL of a 100 U mL⁻¹ enzyme solution in Tris-HCl buffer (50 mmol L⁻¹, pH 9) is added and introduced again in the ultrasonic bath for 30 min at 4 °C. The suspension with the enzyme immobilized was centrifuged at 3000 rpm for 20 min. Subsequently, three washes were performed: two with a 50 mmol L⁻¹ phosphate buffer adjusted to pH 8, and one with a 100 mmol L⁻¹ Tris-HCl buffer to which 100 mmol L⁻¹ NaCl was added and was adjusted to pH 8. Supernatants obtained were stored in the fridge at 4 °C until their use in the measurement of the immobilization effectiveness.

The characterization of the GPx-MNPs complex has been avoided because MNPs and the complex with enzymes have been previously described [32, 34]. After the immobilization of the enzyme, “batch” tests were performed to evaluate the efficiency of the GPx immobilization process on MNPs. These studies consisted in the measure of the fluorescence intensity of the reaction that occurred between HVA (0.1 mmol L⁻¹) and H₂O₂ (0.1 mmol L⁻¹) in presence of GSH (2.5 μmol L⁻¹) and different GPx enzyme activities (0–1 U mL⁻¹). All solutions were prepared in the 50 mmol L⁻¹ Tris-HCl buffer adjusted at pH 9. In all the trials, the signal reduction at the excitation and emission wavelengths of the HVA dimer was monitored. The GPx immobilization efficiency using the fluorimetric method described above let results in an immobilization yield of 92.1 ± 0.5%. The behavior of the immobilized enzyme has been compared to that of the enzyme in solution, with the same activity enzyme immobilized and in solution (0.5 U mL⁻¹). Similar enzyme activity was obtained in both cases, assuming no activity loss by immobilizing the enzyme. The stability of the immobilized enzyme has also been evaluated by monitoring the signals of decreased fluorescence over time. All the tests were conducted under experimental conditions

with different concentrations of HVA (0.1–10 μmol L⁻¹). The stability of the immobilized enzyme was maintained constant for at least 2 months when it was immobilized (activity losses lower than 2%).

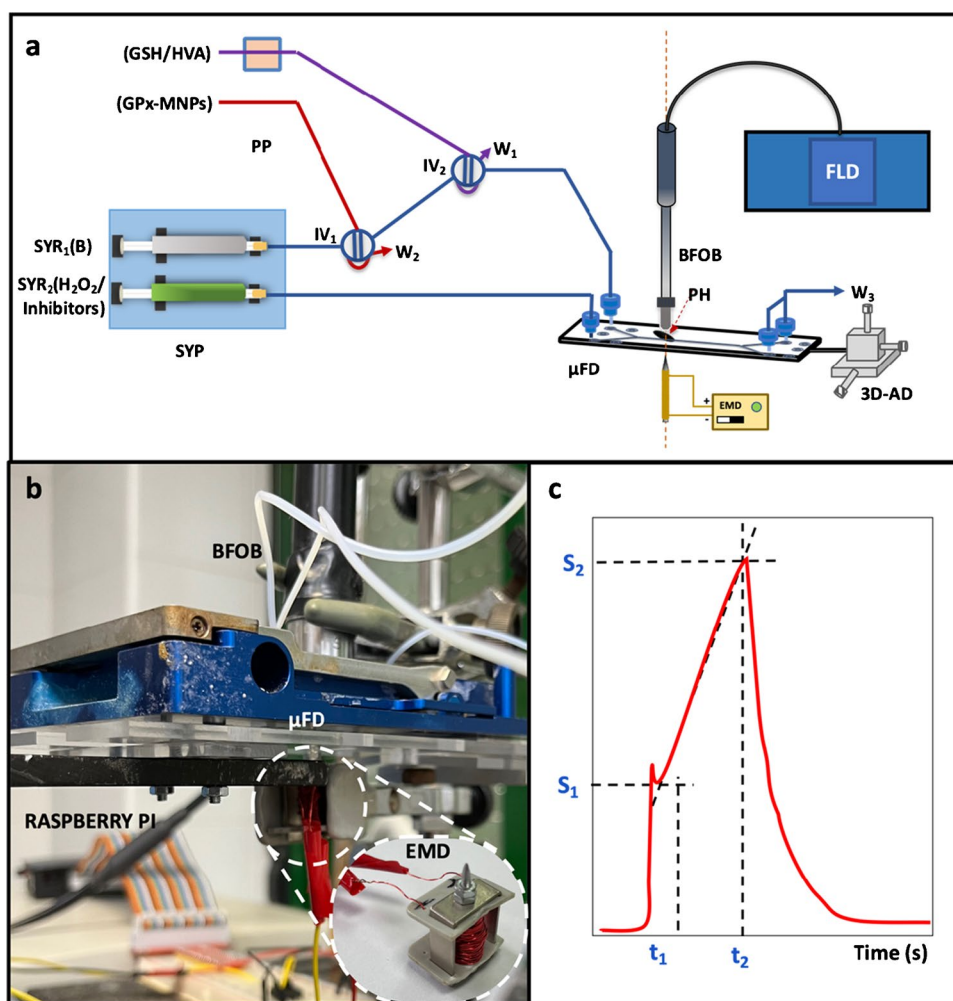
Microfluidic system configuration

The microfluidic size of the system with an on-flow stopped-flow mode was chosen to develop the competitive kinetic reactions. For this purpose, the GPx enzyme was incorporated and retained in the reaction/detection zone of the system as GPx-MNPs complex to form the MREμR. This device acted as a catalytic enzyme reactor but also provides a rapid mixture of the reactants avoiding laminar diffusion. Figure 2a depicts the on-flow stopped-flow microfluidic configuration. Figure 2b shows an image in detail of the coupling of the lab-built electromagnet device used to retain the immobilized enzyme and form the MREμR, as well as the coupling of a BFOB in the reaction/detection zone to monitor the reaction. The control of the electromagnet device has been carried out using the embedded device Raspberry Pi 3 Model 3 with Python commands. The BFOB has been aligned to the reaction/detection zone of the microfluidic device using an x–y–z alignment device. As can be seen, the use of a microfluidic device incorporating two injection valves has been chosen to control the regeneration of the MREμR and introduce simultaneously the two reducing substrates of both analytical (GSH) and indicator (HVA) reactions. H₂O₂ was introduced continuously as the oxidant substrate to both reactions towards the reaction/detection zone. When a GPx inhibitor is required, this was introduced in the same solution with the oxidant substrate.

One first stage was required to introduce a volume of 50 μL solution containing the GPx-MNPs complex through the injection valve (IV₁) to form the MREμR, leaving the enzyme magnetically retained in the optical pathway. This step is required once for all measurements since the enzyme was reused. In the second stage, the injection of the GSH/HVA substrate mixture through injection valve IV₂ into the reaction/detection zone occurred. At an exact previous injection time of 10 s (*t*₁), since the substrates were injected, the flow was stopped, and the kinetic tracking of the enzymatic reaction took place during the stopped time of 120 s (*t*₂), in which a proportional peak corresponding to the development of both competing reactions (enzyme-catalyzed and indicator) was formed. The hydrogen peroxide solution and the inhibitors passed continuously through the system.

The reaction of the HVA with the H₂O₂ catalyzed by GPx caused an increase in the fluorescence due to the HVA dimer, which is monitored in the spectrofluorimeter at the excitation and emission wavelengths of 317 and 425 nm, respectively,

Fig. 2 **a** Diagram of the integrated on-flow stopped-flow microfluidic system used. **b** Detail of the integration of the electromagnet device and the bifurcated fiber optic bundle with the microfluidic device in the reaction/detection zone. **c** Instrumental signals acquired with the stopped-flow microfluidic system. PP denotes peristaltic pump; SYP, syringe pump; SYR₁, syringe to introduce buffer solution; SYR₂, syringe to introduce H₂O₂ and inhibitor compounds; IV₁, injection valve for the GPx-MNPs complex solution; IV₂, injection valve for the mixture GSH/HVA solution; μ FD, microfluidic device; BFOB, bifurcated fiber optic bundle; PH, pinhole; EMD, electromagnet device; 3D-AD, x-y-z alignment device; FLD, fluorimetric detector; W₁, W₂, and W₃ waste; S₁ and S₂, signals after the injection and at the end of the kinetic curve; t₁ and t₂, injection and stopped time



using an ex/em slits rate of 5/5 with PMT gain of 950 V. Two types of signals were processed: (a) net signals obtained as the difference between the absence (I_0) and the presence (I) of GSH, being each one the difference between the end (S_2) and the beginning (S_1) of the kinetic curve; and (b) kinetic signals of reaction rates. The signals acquired, as shown in Fig. 2b, showed the typical stopped-flow signal, whose intensity decayed proportionally to the GSH concentration introduced since HVA and GSH competed to reduce H₂O₂. When the study of inhibitors was carried out, their presence induced a signal increase due to inhibiting the glutathione reduction. In this case, the type of enzymatic inhibition was studied thanks to the double reciprocal representation established by Lineweaver–Burk, and the concentration of those inhibitors was determined in different samples.

Sample analysis

The method was applied to determine three different inhibitors of the GPx enzyme, such as Hg(II), Cu(II), and

t-butyl hydroperoxide. These compounds were analyzed in samples of different natures, such as tap water, well water, whole milk, and edible oil, the last two obtained from supermarkets. Sample pretreatment was carried out as follows [35]. The milk samples were pretreated by mixing 20 mL of each sample with 20 mL of 20% trichloroacetic acid solution, stirred for 40 min, and subjected to centrifugation at 4 °C for 15 min at 11,830 × g. Obtained supernatants were collected and filtered through a 0.2 μm membrane, followed by dilution fivefold with Tris–HCl buffer (50 mmol L⁻¹, pH 9). The oil samples were weighted (15 g) and homogenized in 75 mL n-hexane, the mixture was evaporated at 60 °C using a rotary evaporator, and the dried residue was dissolved in 7.5 mL of 5% chloroform. In both cases, the resulting extract solutions were adequately diluted with Tris–HCl buffer for their introduction into the flow system. Two dilution factors were used, 1:100 for the oil samples and 1:10 for the milk samples. The water samples did not need pretreatment, and no dilution was performed in them.

Results and discussion

Study of the variables involved in the developed system

Table 1 summarizes the instrumental, physical, hydrodynamic, and chemical variables studied, using the univariate method, and performing at least three repetitions for each assay, the ranges assayed, and the values chosen. All measurements were studied using two GSH concentrations, 1 and 5 $\mu\text{mol L}^{-1}$, and 0.5 U mL^{-1} activity of the immobilized GPx enzyme. The net signal of the fluorescence intensity corresponding to the $I_0 - I$ differences was selected as the measurement parameter, the intervals tested, and the optimal values, or those adopted due to compromise with the enzymatic and instrumental system.

The study of the instrumental variables was carried out with the spectroscopic study of the HVA indicator reaction. The focus distance of the fiber optic bundle and the pinhole adapted to focus excitation beam at the microfluidic channel were set up to obtain the best signal from the MRE μ R. The power and the length of the electromagnet device inserted to retain the GPx-MNPs complex were studied to obtain the smallest reactor with the maximum enzymatic capacity. The optimal temperature influence was achieved at 30 °C, and values above this temperature caused denaturation of the enzyme. Concerning the hydrodynamic variables, the flow had a significant influence to provide the rapid displacement of the reagents to the reaction/detection zone.

Figure 3a shows the flow rate studied, obtaining the best results with a 40 $\mu\text{L min}^{-1}$ flow rate.

As already mentioned, the microfluidic configuration included two injection valves. IV₁ incorporated the GPx-MNPs complex to form the MRE μ R, choosing an injection volume of 50 μL to retain as much of the immobilized enzyme as possible and to obtain a short segment of MRE μ R to avoid clogging problems. A 1:5 diluted suspension in phosphate buffer (50 mmol L^{-1} , pH 7.4) was incorporated. Concerning IV₂, the reactants involved in enzymatic and indicator reactions were introduced, with a volume of 5 μL to obtain a narrow peak. Figure 3b and c show the influence of the previous time and the stopped time, observing the best signals at the optimal values of 10 and 120 s, respectively.

Furthermore, to study the chemical variables, a kinetic study of the two oxidation reactions with the GSH and HVA substrates in presence of H_2O_2 was performed. The best results were obtained using Tris-HCl buffer 50 mmol L^{-1} adjusted to pH 9. One of the fundamental steps was the conversion of GSH to GSSG, since the H_2O_2 was consumed, and the rest reacted in the indicator reaction with HVA. For this, enough H_2O_2 must be added so that once it reacts with GSH, there was enough left to give the indicator reaction. As shown in Fig. 3d, for levels of H_2O_2 concentration higher than 10 $\mu\text{mol L}^{-1}$, the net signal was not modified. The HVA concentration should be studied to obtain an extended range of linearity for the method without the saturation of the indicator reaction. Figure 3e depicts the best signal acquired with 2.5 $\mu\text{mol L}^{-1}$ for HVA.

Table 1 Optimization of variables

Type of variable	Variable	Range studied	Optimal value
Instrumental	λ_{ex} , nm	200–800	317
	λ_{em} , nm	200–800	425
	Excitation slits, nm	1–10	5
	Emission slits, nm	1–10	5
	PMT power, V	600–950	950
	Focused length, mm	2–20	10
	Pinhole diameter, mm	0.1–3	1.5
	Electromagnet device power, V	–	6
	Electromagnet device tip length, mm	1–10	5
Physical	Temperature, °C	25–60	30
Hydrodynamic	Flow rate, $\mu\text{L min}^{-1}$	10–100	40
	Injection volume IV ₁ , μL	10–50	50
	Injection volume IV ₂ , μL	1–5	5
	Previous time, s	5–20	10
	Stopped time, s	50–200	120
Chemical	[Tris-HCl], mmol L^{-1}	10–100	50
	pH	6–9	9
	GPx-MPNs dilution	1/2–1/10	1/5
	[H_2O_2], $\mu\text{mol L}^{-1}$	0.1–10	10
	[HVA], $\mu\text{mol L}^{-1}$	1–10	2.5

Fig. 3 Influence of some experimental variables of the stopped-flow microfluidic system: **a** flow rate, **b** previous time, **c** stopped time, **d** $[H_2O_2]$, and **e** [HVA]. The net signal ($I_0 - I$) obtained is shown for two concentrations of GSH, (1) 1 and (2) $5 \mu\text{mol L}^{-1}$

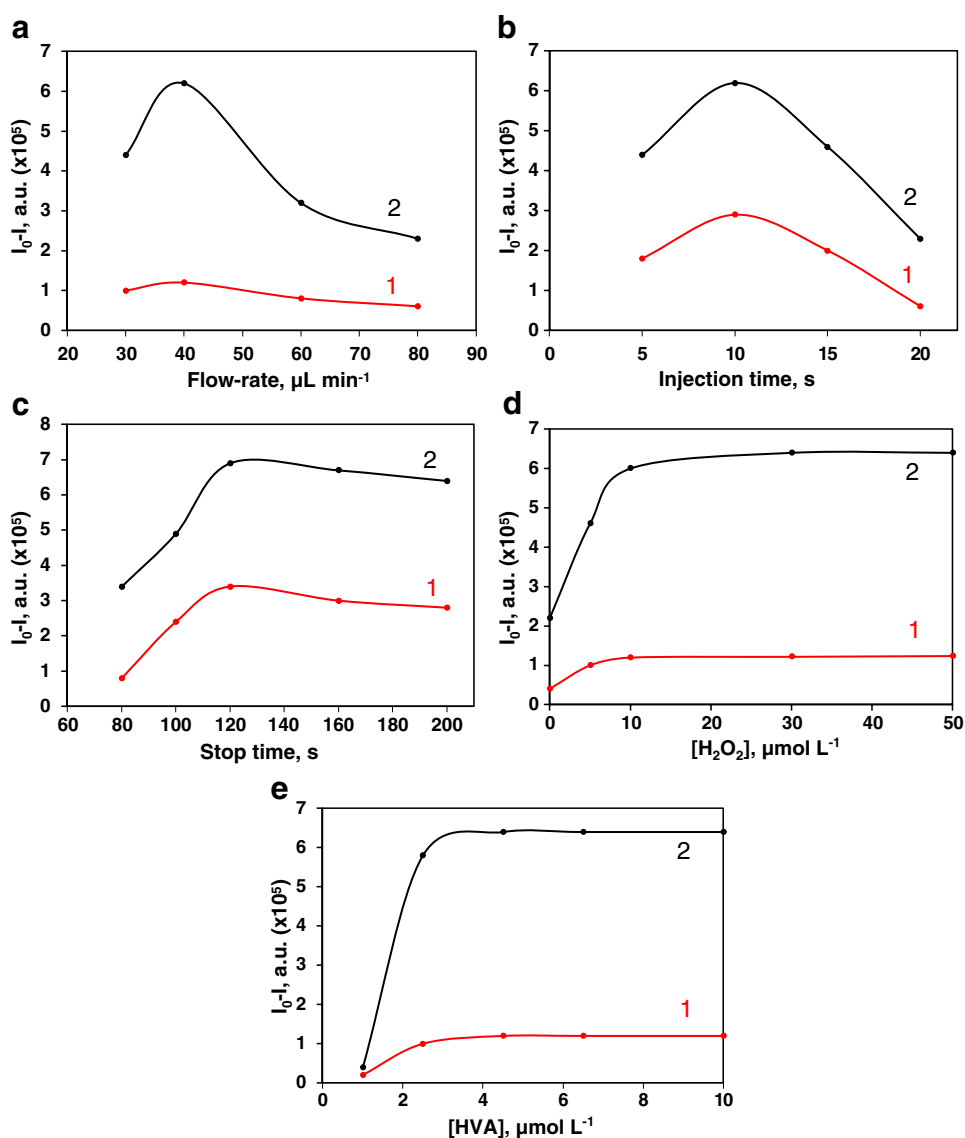


Table 2 Kinetic-enzymatic parameters that define the GPx enzyme inhibition

Inhibitor type	[Inhibitor], $\mu\text{mol L}^{-1}$	Lineweaver–Burk equation			Kinetic parameters		K_I , $\mu\text{mol L}^{-1} \text{s}^{-1}$
		Slope	Intercept	r^2	K_M , $\mu\text{mol L}^{-1}$	v_{MAX} , $\mu\text{mol L}^{-1} \text{s}^{-1}$	
Hg(II)	1	0.01	0.0015	0.998	46.98	712.71	749.18
	5	0.064	0.0014	0.997	71.42	714.32	1023.30
	10	0.128	0.0013	0.966	91.66	720.09	1323.80
Cu(II)	1	1.59	0.002	0.991	649.71	153.98	1129.65
	5	5.35	0.003	0.992	744.32	141.49	4234.98
	10	1.33	0.0007	0.994	2530.09	149.66	23,190.9
t-butyl hydroperoxide	1	2.27	0.06	0.998	580.09	158.98	117.09
	5	7.37	0.13	0.987	599.65	138.09	293.09
	10	15.76	0.04	0.965	601.65	121.98	2803.45

GPx enzyme inhibition study in the microfluidic system

The study of the potential inhibition effect of two metals (Cu(II) and Hg(II)) and t-butyl hydroperoxide was carried out to demonstrate the usefulness of the stopped-flow microfluidic system. In all cases, the representation of the initial rate (v_i) using the double reciprocal method of Lineweaver–Burk was established. The determination of the inhibition constant of each specie was carried out at three concentrations of each inhibitor compound (1, 5, and 10 $\mu\text{mol L}^{-1}$), and this study allowed knowing the inhibition model of each tested compound. The results obtained for each inhibitor compound are listed in Table 2. As can be deduced, the metals Hg(II) and Cu(II) behave as competitive inhibitors because the v_{MAX} values remained constant (estimated value of $715.7 \pm 3.6 \mu\text{mol L}^{-1} \text{s}^{-1}$) and K_M increased depending on the metal concentration. In the case of t-butyl hydroperoxide, the values of K_M (estimated value of $593.79 \pm 7.98 \mu\text{mol L}^{-1}$) remained practically constant, and there was a slight decrease in v_{MAX} at increasing inhibitor concentration, confirming the non-competitive inhibition. The inhibition observed showed similar results to those obtained in the literature [24, 30, 31], meaning that the immobilization of the enzyme in MNPs does not affect the inhibition response of the enzyme.

Features of the method

Once the inhibition effect has been demonstrated, the method was applied to determine these inhibition compounds. For that, some calibration graphs were found using the optimal values obtained in the previous section and using net signals. A calibration graph was obtained to determine the substrate, and other ones were acquired to determine Cu(II), Hg(II), and t-butyl hydroperoxide. Table 3 shows the equation parameters of the calibration graphs, the concentration

Table 4 Application of the method

Sample	Studied compound	Found ^a	Recovery ^{a,b}	
			1st add	2nd add
Tap water	Hg(II)	n.d. ^c	98.3	94.8
	Cu(II)	n.d. ^c	95.2	90.9
Well water	Hg(II)	n.d. ^c	94.6	93.7
	Cu(II)	n.d. ^c	99.4	96.2
Whole milk	t-butyl hydroperoxide	0.9 ± 0.02	95.5	92.8
Olive oil	t-butyl hydroperoxide	8.6 ± 0.05	93.4	89.9
Sunflower oil	t-butyl hydroperoxide	28.9 ± 0.09	94.2	88.7

^aMean value of three experiments

^b1st adds, 1 $\mu\text{mol L}^{-1}$ and 2nd add, 5 $\mu\text{mol L}^{-1}$

^cNon-detected

ranges studied, the detection limit calculated according to the IUPAC recommendations, and the precision expressed in terms of relative standard deviation percentage (RSD%).

Application of the method

The method was applied to determine some inhibitors of the GPx enzyme in environmental and food samples, such as tap water, well water, milk, and edible oil, to establish the applicability of the on-flow stopped-flow microfluidic system developed using the procedure described above. The pretreated and diluted samples were first analyzed to verify the presence of the inhibition compounds. However, some of the studied compounds were not contained in the samples. Therefore, a recovery study was carried out by adding two different amounts of each compound to each sample to achieve final analyte concentrations of 1 and 5 $\mu\text{mol L}^{-1}$. Table 4 shows the recovery values obtained, ranging between 88.7 and 99.4%. The results confirmed that the developed method was highly reliable and applicable to Hg(II), Cu(II), and t-butyl hydroperoxide detection in real samples.

Table 3 Features of the method

	Equation parameters ^a			LOD, $\mu\text{mol L}^{-1}$	Linear range, $\mu\text{mol L}^{-1}$	RSD, % ^b	
	Slope	Intercept	r^2			Max. error	Min. error
Glutathione	$2.9 \cdot 10^4$ ($\pm 2 \cdot 10^2$)	$4.5 \cdot 10^5$ ($\pm 1.6 \cdot 10^4$)	0.9954	0.1	0.45–10	3.9	0.6
Hg (II)	$3.1 \cdot 10^3$ (± 54.5)	$3.1 \cdot 10^3$ ($\pm 3.2 \cdot 10^2$)	0.9969	0.031	0.1–10	5.4	1.1
Cu (II)	$1.7 \cdot 10^4$ ($\pm 4.3 \cdot 10^2$)	$1.9 \cdot 10^4$ ($\pm 2.7 \cdot 10^2$)	0.9993	0.049	0.2–10	4.3	0.9
t-butyl hydroperoxide	$3.1 \cdot 10^4$ ($\pm 3.1 \cdot 10^2$)	$3.6 \cdot 10^4$ ($\pm 2.1 \cdot 10^2$)	0.9902	0.019	0.06–10	4.8	0.8

^a $y = (I_0 - I)$ and $x = [\text{GSH}], \mu\text{mol L}^{-1}$

^bRSD% values achieved at the maximum and minimum error zones (0.5 $\mu\text{mol L}^{-1}$ and 5 $\mu\text{mol L}^{-1}$, respectively)

Conclusions

A stopped-flow microfluidic device has been developed successfully using a magnetically retained enzymatic microreactor to study kinetic-enzymatic parameters and the inhibitory properties of some compounds in the enzyme. For that, glutathione peroxidase (GPx) has been immobilized on magnetic nanoparticles (MNPs) to form the GPx-MNPs complex to be retained in the reaction/detection zone of the microfluidic system. A chemical system has been proposed for monitoring the GPx enzymatic activity in the absence and presence of inhibitors, based on the combination of two oxidation reactions in which the enzyme substrate, glutathione, and homovanillic acid competed for their interaction with H₂O₂. The product of the homovanillic acid reaction was a fluorescent compound that allowed the quantification of glutathione or inhibitor compounds. Finally, developing a microfluidic system based on the stopped-flow mode allowing enzyme retention is a useful tool to characterize enzymatic systems and study the behavior of enzymatic inhibitors with low enzyme consumption.

Author contribution V. Román-Pizarro: conceptualization; methodology; formal analysis; investigation; writing—review and editing; visualization; supervision. A. Carrión-Escudero: methodology; formal analysis; investigation; writing—original draft. Á. Écija-Arenas: writing—review and editing; supervision. J. M. Fernández-Romero: conceptualization; methodology; investigation; resources; writing—review and editing; visualization; supervision; project administration; funding acquisition.

Funding Funding for open access publishing: Universidad de Córdoba/CBUA. This work was supported by the Operative Framework Funding FEDER-Andalucía 2014–2020 Program (ref. UCO-1263679 and UCO-180001). The author AEA received funding from this program. The authors also received initial financial support from the Spanish MICINN (Ministerio de Ciencia e Innovación) (Grant No. CTQ2012-32941/BQU) and the Junta de Andalucía (Grant No. PO9-FQM-4933).

Declarations

Conflict of interest The authors declare no competing interests.

Open Access This article is licensed under a Creative Commons Attribution 4.0 International License, which permits use, sharing, adaptation, distribution and reproduction in any medium or format, as long as you give appropriate credit to the original author(s) and the source, provide a link to the Creative Commons licence, and indicate if changes were made. The images or other third party material in this article are included in the article's Creative Commons licence, unless indicated otherwise in a credit line to the material. If material is not included in the article's Creative Commons licence and your intended use is not permitted by statutory regulation or exceeds the permitted use, you will need to obtain permission directly from the copyright holder. To view a copy of this licence, visit <http://creativecommons.org/licenses/by/4.0/>.

References

- Vakh C, Koronkiewicz S, Kalinowski S, Moskvina L, Bulatov A. An automatic chemiluminescence method based on the multi-pumping flow system coupled with the fluidized reactor and direct-injection detector: determination of uric acid in saliva samples. *Talanta*. 2017;167:725–32. <https://doi.org/10.1016/j.talanta.2017.02.009>.
- Sun Q, Tu J, Yaroshenko I, Kirsanov D, Legin A, Wang P. Enzymatic determination of urinary citrate based on flow injection system using NUV spectroscopy and PLS regression. *Sens Actuators B Chem*. 2017;251:1050–8. <https://doi.org/10.1016/j.snb.2017.04.027>.
- Amatatongchai M, Sroysee W, Chairam S, Nacapricha D. Amperometric flow injection analysis of glucose using immobilized glucose oxidase on nano-composite carbon nanotubes-platinum nanoparticles carbon paste electrode. *Talanta*. 2017;166:420–7. <https://doi.org/10.1016/j.talanta.2015.11.072>.
- Trojanowicz M. Flow-injection analysis as a tool for determination of pharmaceutical residues in aqueous environment. *Talanta*. 2012;96:3–10. <https://doi.org/10.1016/j.talanta.2011.12.081>.
- Ji Q, Wang B, Tan J, Zhu L, Li L. Immobilized multienzymatic systems for catalysis of cascade reactions. *Process Biochem*. 2016;51:1193–203. <https://doi.org/10.1016/j.procbio.2016.06.004>.
- Ren S, Li C, Jiao X, Jia S, Jiang Y, Bilal M, Cui J. Recent progress in multienzymes co-immobilization and multienzyme system applications. *Chem Eng J*. 2019;373:1254–78. <https://doi.org/10.1016/J.CEJ.2019.05.141>.
- Guzik U, Hupert-Kocurek K, Wojcieszynska D (2014) Immobilization as a strategy for improving enzyme properties-application to oxidoreductases. *Molecules* 2014, Vol 19, Pages 8995–9018 19:8995–9018. <https://doi.org/10.3390/MOLECULES19078995>
- Kouassi GK, Irudayaraj J, McCarty G. Examination of cholesterol oxidase attachment to magnetic nanoparticles. *J Nanobiotechnology*. 2005;3:1. <https://doi.org/10.1186/1477-3155-3-1>.
- Huang S, Li C, Cheng Z, Fan Y, Yang P, Zhang C, Yang K, Lin J. Magnetic Fe₃O₄ mesoporous silica composites for drug delivery and bioadsorption. *J Colloid Interface Sci*. 2012;376:312–21. <https://doi.org/10.1016/j.jcis.2012.02.031>.
- Fortes CCS, Daniel-da-Silva AL, Xavier AMRB, Tavares APM. Optimization of enzyme immobilization on functionalized magnetic nanoparticles for laccase biocatalytic reactions. *Chem Eng Process*. 2017;117:1–8. <https://doi.org/10.1016/j.cep.2017.03.009>.
- Xu K, Chen X, Zheng R, Zheng Y. Immobilization of multi-enzymes on support materials for efficient biocatalysis. *Front Bioeng Biotechnol*. 2020;8:660. <https://doi.org/10.3389/FBIOE.2020.00660/BIBTEX>.
- Weaver K, Skouta R (2022) The selenoprotein glutathione peroxidase 4: from molecular mechanisms to novel therapeutic opportunities. *Biomedicine* 2022, Vol 10, Page 891 10:891. <https://doi.org/10.3390/BIOMEDICINES10040891>
- Zhang J, Hao H, Wu X, Wang Q, Chen M, Feng Z, Chen H. The functions of glutathione peroxidase in ROS homeostasis and fruiting body development in *Hypsizygus marmoreus*. *Appl Microbiol Biotechnol*. 2020;104:10555–70. <https://doi.org/10.1007/S00253-020-10981-6>.
- Araujo ARTS, Saraiva MLMFS, Lima JLFC. Determination of total and oxidized glutathione in human whole blood with a sequential injection analysis system. *Talanta*. 2008;74:1511–9.
- Satoh I, Arakawa S, Okamoto A. Flow injection determination of glutathione with amperometric monitoring of the enzymatic reaction. *Anal Chim Acta*. 1988;214:415–9.

16. Satoh I, Arakawa S, Okamoto A. Calorimetric flow-injection determination of glutathione with enzyme-thermistor detector. *Sensors and Actuators B*. 1991;5:245–7.
17. Cherry JR, Fidantsef AL. Directed evolution of industrial enzymes: an update. *Curr Opin Biotechnol*. 2003;14:438–43. [https://doi.org/10.1016/S0958-1669\(03\)00099-5](https://doi.org/10.1016/S0958-1669(03)00099-5).
18. Abdollahi K, Yazdani F, Panahi R. Covalent immobilization of tyrosinase onto cyanuric chloride crosslinked amine-functionalized superparamagnetic nanoparticles: synthesis and characterization of the recyclable nanobiocatalyst. *Int J Biol Macromol*. 2017;94:396–405. <https://doi.org/10.1016/j.ijbiomac.2016.10.058>.
19. Durán N, Rosa MA, D'annibale A, Gianfreda L. Enzyme and Microbial Technology 31 (2002) 907–931 Review Applications of laccases and tyrosinases (phenoloxidases) immobilized on different supports: a review. *Enzyme Microb Technol*. 2002;31:907–31.
20. Majeau JA, Brar SK, Tyagi RD. Laccases for removal of recalcitrant and emerging pollutants. *Bioresour Technol*. 2010;101:2331–50. <https://doi.org/10.1016/j.biortech.2009.10.087>.
21. Hyeon JE, Shin SK, Han SO. Design of nanoscale enzyme complexes based on various scaffolding materials for biomass conversion and immobilization. *Biotechnol J*. 2016;11:1386–96. <https://doi.org/10.1002/biot.201600039>.
22. Kluchova K, Zboril R, Tucek J, Pecova M, Zajoncova L, Safarik I, Mashlan M, Markova I, Jancik D, Sebel M, Bartonkova H, Bellesi V, Novak P, Petridis D. Superparamagnetic maghemite nanoparticles from solid-state synthesis - their functionalization towards peroral MRI contrast agent and magnetic carrier for trypsin immobilization. *Biomaterials*. 2009;30:2855–63. <https://doi.org/10.1016/j.biomaterials.2009.02.023>.
23. Dobritzsch D, Grancharov K, Hermsen C, Krauss G-J, Schaumlöf-fel D. Inhibitory effect of metals on animal and plant glutathione transferases. *J Trace Elem Med Biol*. 2020;57:48–56. <https://doi.org/10.1016/j.jtemb.2019.09.007i>.
24. Ekinçi D, Şentürk M. Assessment of metal inhibition of antioxidant enzyme glutathione reductase from rainbow trout liver. *J Enzyme Inhib Med Chem*. 2013;28:11–5. <https://doi.org/10.3109/14756366.2011.615745>.
25. Alía M, Ramos S, Mateos R, Bravo L, Goya L. Response of the antioxidant defense system to tert-butyl hydroperoxide and hydrogen peroxide in a human hepatoma cell line (HepG2). *J Biochem Mol Toxicol*. 2005;19:119–28. <https://doi.org/10.1002/JBT.20061>.
26. Alisik M, Neselioglu S, Erel O. A colorimetric method to measure oxidized, reduced and total glutathione levels in erythrocytes. *Journal of Laboratory Medicine*. 2019;43:269–77. <https://doi.org/10.1515/LABMED-2019-0098/MACHINEREADABLECITATION/RIS>.
27. Paital B (2014) A modified fluorimetric method for determination of hydrogen peroxide using homovanillic acid oxidation principle. *Biomed Res Int* 2014;342958. <https://doi.org/10.1155/2014/342958>.
28. Guillaubault GG, Brignac P Jr, Zimmer M. Homovanillic acid as a fluorometric substrate for oxidative enzymes. *Anal Chem*. 1968;40:190–6.
29. Zhang W, Ye W, Wang Y, Yan Y (2022) Microfluidic fabrication of tunable alginate-based microfibers for the stable immobilization of enzymes. *Biotechnol J* 17:;. <https://doi.org/10.1002/BIOT.202200098>.
30. Splittgerber AG, Tappel AL. Inhibition of glutathione peroxidase by cadmium and other metal ions. *Arch Biochem Biophys*. 1979;197:534–42.
31. Singh BG, Bag PP, Kumakura F, Iwaoka M, Priyadarsini KI. Role of substrate reactivity in the glutathione peroxidase (gpx) activity of selenocystine. *Bull Chem Soc Jpn*. 2010;83:703–8. <https://doi.org/10.1246/bcsj.20090348>.
32. Écija-Arenas Á, Román-Pizarro V, Fernández-Romero JM. Usefulness of hybrid magnetoliposomes for aminoglycoside antibiotic residues determination in food using an integrated microfluidic system with fluorometric detection. *J Agric Food Chem*. 2021;69:6888–96. <https://doi.org/10.1021/acs.jafc.1c01571>.
33. Saiyed ZM, Sharma S, Godawat R, Telang SD, Ramchand CN. Activity and stability of alkaline phosphatase (ALP) immobilized onto magnetic nanoparticles (Fe₃O₄). *J Biotechnol*. 2007;131:240–4. <https://doi.org/10.1016/J.JBIOTEC.2007.06.017>.
34. Román-Pizarro V, Ramírez-Gutiérrez M, Gómez-Hens A, Fernández-Romero JM (2020) Usefulness of magnetically-controlled MNPs-enzymes microreactors for the fluorimetric determination of total cholesterol in serum. *Talanta* 208:120426. <https://doi.org/10.1016/j.talanta.2019.120426>
35. Román-Pizarro V, Gómez-Hens A, Fernández-Romero JM. Applicability of fluorescent hybrid magnetoliposomes for the determination of reactive oxygen compounds in food. *Food Anal Methods*. 2018;11:2376–83. <https://doi.org/10.1007/s12161-018-1220-3>.

Publisher's note Springer Nature remains neutral with regard to jurisdictional claims in published maps and institutional affiliations.